Polymer 285 (2023) 126382

Contents lists available at ScienceDirect

Polymer

journal homepage: www.elsevier.com/locate/polymer

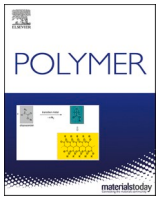

Tunable thermal property of poly(styrene-*alt*-phenylmaleimide)-based alternating copolymers through mediated hydrogen bonding strength

Wei-Ting Du [a], Shiao-Wei Kuo [a,b,*]

[a] Department of Materials and Optoelectronic Science, Center of Crystal Research, National Sun Yat-Sen University, Kaohsiung, 804, Taiwan
[b] Department of Medicinal and Applied Chemistry, Kaohsiung Medical University, Kaohsiung, 807, Taiwan

A B S T R A C T

The glass transition temperature (T_g) value of poly(styrene–*alt*–hydroxyphenylmaleimide) (poly(S–*alt*–HPMI)) is much higher than poly(styrene–*co*–vinyl phenol) due to the presence of the maleimide unit in poly(S–*alt*–HPMI) and its intramolecular screening effect result in a substantially higher T_g value. In this study, our focus was revolved about the impact of *para*–OH groups with different combinations and their influence on their T_g values. To achieve this, six alternating copolymers using free radical copolymerization were synthesized and performed them to comprehensive characterizations including Fourier–transform infrared spectroscopy (FTIR), nuclear magnetic resonance (NMR), matrix–assisted laser desorption ionization/time of flight (MALDI–TOF) mass spectrometry, and gel permeation chromatography (GPC), which were crucial in confirming the chemical structures and sequence distributions of these alternating copolymers. We employed the 2D–FTIR spectral analysis method, comparing copolymers with OH groups on the styrene unit, the phenylmaleimide unit, or both to understand the diverse effects of OH groups. Furthermore, we compared these findings with acetoxy–styrene (AS) derivative copolymers and poly(styrene–*alt*–phenylmaleimide) (poly(S–*alt*–PMI)), which lacks any hydrogen bonded donor units. As a result, this work not only contributes to a valuable understanding of the role of hydrogen bonding in polymeric materials but also provides deeper insights for designing polymers with tunable thermal properties by strategic placement of OH groups.

1. Introduction

Hydrogen bonding is a fundamental scientific concept and received in the development of new materials that has led to groundbreaking advancements in various materials such as metal, covalent or hydrogen bonded–organic frameworks, epoxy, benzoxazine, nylon and thermoplastic polyurethane (TPU) [1–7]. It is also fascinating to find that its interaction strength could be mediated through the design of their chemical structures. The intermolecular hydrogen bonding strength has opened up new avenues for polymer engineering, allowing for the design of customized functionalities and properties. As a result, hydrogen bonding is still remained the ongoing field of innovation and exploration in the pursuit of advanced polymeric materials [8–10].

According to Painter and Coleman results, they found the decrease in the self–association equilibrium constant (K_B) of phenolic units with attached methyl, isopropyl or *tert*–butyl groups due to steric hindrance. Furthermore, they also observed that poly(vinyl phenol) (PVPh) displayed a higher K_B value compared to poly(hexafluoro–2–hydroxy–2–propyl styrene), which was attributed to the acidity of the hydroxyl groups present on the aromatic ring and the carbon atom with sp^3 hybrid orbital [11]. In determining the hydrogen bonding interaction of polymer pairs between a hydrogen bonding donor with a hydrogen–bonded acceptor such as poly(caprolactone) (PCL), the relative (K_A/K_B) of the inter/self–association equilibrium constant ratio is more important than considering only K_A or K_B individually where K_A is the inter–association equilibrium constant between hydroxyl (OH) and carbonyl (C═O) groups. When comparing the hydrogen bonding interactions of different hydrogen bonding donor polymers with PCL, the order of K_A/K_B is as follows: phenolic/PCL > PVPh/PCL > phenoxy/PCL because of different acidic properties of these three bonding donor polymers [12].

Recently, there has been much advancement in the development of synthetic polymers. The arrangement of monomer sequences in copolymers has also proven to be crucial in the hydrogen bonding polymer pairs [13–15]. For example, it is possible to find self–assembled ordered morphological transitions as by blending poly(styrene–*b*–4–vinylpyridine) [poly(S–*b*–4VP)] with poly(VPh–*b*–methyl methacrylate) [poly(VPh–*b*–MMA)] in specific ratios through mediated by hydrogen bonding interactions [16]. An interesting observation is that the intermolecular hydrogen bonding interaction in poly(VPh–*co*–MMA) random copolymer is stronger than those of poly(VPh–*b*–MMA) diblock copolymers and the PVPh/PMMA binary blends

* Corresponding author. Department of Materials and Optoelectronic Science, Center of Crystal Research, National Sun Yat-Sen University, Kaohsiung, 804, Taiwan.
E-mail address: kuosw@faculty.nsysu.edu.tw (S.-W. Kuo).

https://doi.org/10.1016/j.polymer.2023.126382
Received 1 June 2023; Received in revised form 29 August 2023; Accepted 24 September 2023
Available online 25 September 2023
0032-3861/© 2023 Elsevier Ltd. All rights reserved.

[17] because of the chain connectivity [18] and the intramolecular screening effect [19–21]. In homopolymers with OH groups, the repeating units can interact with neighboring OH groups, thereby reducing the number of OH groups available for intermolecular hydrogen bonding with hydrogen bonding acceptor polymers. However, the incorporation of units lacking hydrogen bonding donors (inert segment) in the random copolymers could decrease the K_B value and thus the increase of K_A/K_B ratio. Taking these findings into consideration, we have designed and synthesized the alternating copolymer of poly(S–*alt*–HPMI), which displayed significantly higher T_g value with the strong inter–chain hydrogen bonding interaction as compared with conventional polymers [22]. Moreover, the poly(S–*alt*–HPMI) and poly (S–*co*–VPh) copolymers blending with poly(vinyl pyrrolidone) (PVP) binary blends demonstrated a positive deviation from a linear equation, suggesting a clear occurrence of intermolecular hydrogen bonding interactions within these blends [22–24].

In this study, we designed and synthesized six different alternating copolymers as shown in Scheme 1 by using the hydrogen bonding donors of the VPh and the HPMI units, while the styrene unit and PMI unit acted as the inert diluent segment. To investigate their chemical structures, hydrogen bonding interactions and sequence distributions, we performed characterization techniques including FTIR, NMR, and MALDI–TOF MS analyses. Poly(VPh–*alt*–HPMI) was synthesized to investigate whether the intramolecular screening effect occurs, even when the lengths of the repeating units are different. The thermal properties of these alternating copolymers were determined by using differential scanning calorimetry (DSC), thermogravimetric analysis (TGA), and a two–dimensional FTIR spectral analysis method with temperature disturbance. The aim was to understand the correlation between the thermal properties and intermolecular interactions in these alternative copolymers.

2. Experimental section

2.1. Materials

Styrene (99%), maleic anhydride (98%), and were acquired from Alfa Aesar. Azobisisobutyronitrile (AIBN), ammonium ethanoate, and *p*–toluenesulfonic acid monohydrate ($TsOH{\cdot}H_2O$) were obtained from SHOWA. Methanol (MeOH), tetrahydrofuran (THF), aniline, and toluene were acquired from Acros Organics. 4–Acetoxystyrene, *N*, *N*–dimethylformamide (DMF), and cyclohexane were purchased from TCI.

2.2. N–phenylmaleimide (PMI) and 4–hydroxyphenylmaleimide (HPMI) monomers

Maleic anhydride (4.432 g, 45.2 mmol) and aniline (4.189 g, 45.0 mmol) was used to prepare PMI monomer that were firstly dissolved in toluene (40 mL) and DMF (20 mL) in the 150 mL two–neck round–bottom flask. The flask was placed in an ice bath and stirred for half an hour. Then, a solution of $TsOH{\cdot}H_2O$ (0.490 g, 2.6 mmol) in DMF (5 mL) was added dropwise to the flask. The reaction mixture was refluxed overnight under a nitrogen (N_2) atmosphere. After completing the reaction, the resulting solution was chilled in an ice bath for 30 min and then cold water was poured into the solution. The formed precipitate was filtered off, washed with distilled water, and recrystallized using cyclohexane, and dried in a vacuum oven at 50 °C for 2 days to obtain brown solid. Yield: 36.2%; FTIR (KBr, cm^{-1}): 1714 (C═O), 3000–3220 (sp^2 C–H); ^1H NMR (500 MHz, DMSO–d_6, δ, ppm): 7.18 (s, 2H, C**H**═C**H**), 7.32 (m, 2H, Ar**H**), 7.39 (m, 1H, Ar**H**), 7.48 (m, 2H, Ar**H**); ^{13}C NMR (500 MHz, DMSO–d_6, δ, ppm): 127.49, 128.42, 129.56, 132.26 (Ar**C**), 135.37 (**C**H═**C**H), 170.84 (**C**═O). The synthesis of 4–hydroxyphenylmaleimide

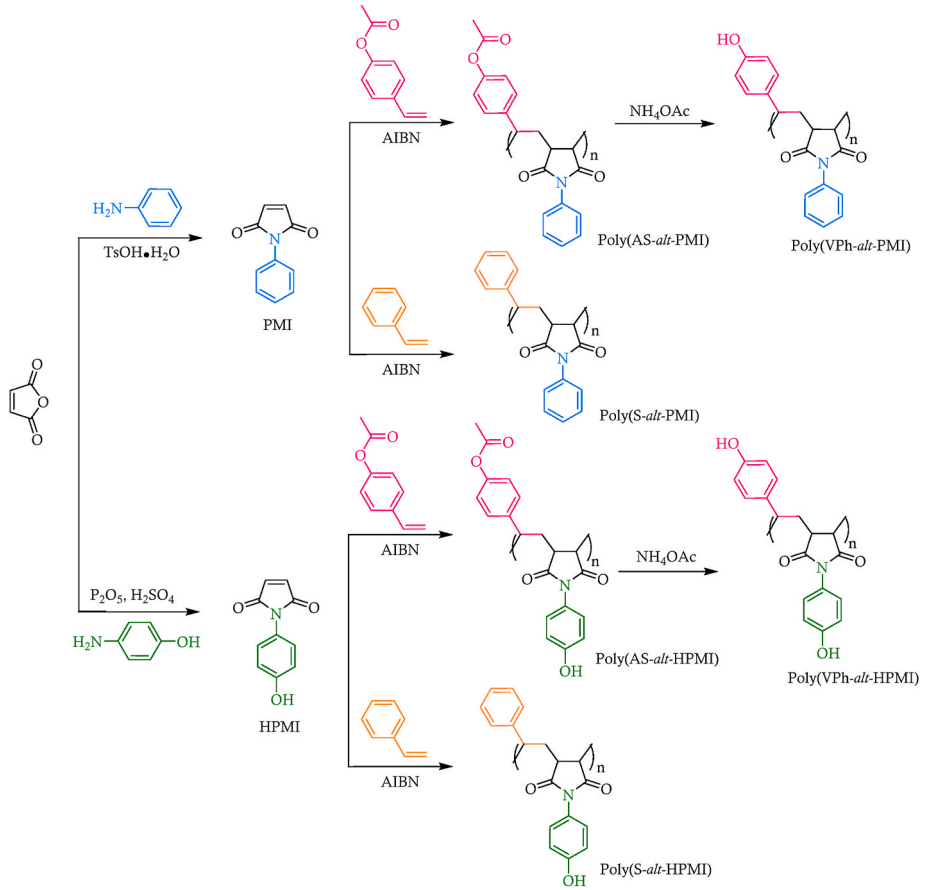

Scheme 1. The synthesis of maleimide derivatives and their corresponding alternating copolymers.

(HPMI) has been mentioned previously [22].

2.3. Polymerization of poly(S–alt–PMI) copolymers

In a 50 mL two–necked round–bottom flask, PMI (0.952 g, 5.5 mmol) and AIBN (5 wt%) were used. Dry THF (15 mL) and styrene (5.5 mmol) were then injected into the flask and the mixture was stirred under N_2 at 70 °C for 1 day. To quench the reaction, the solution was exposed to air for 30 min. The solution was added dropwise into the cold MeOH and then the solid was reprecipitated. The solid was dried for 2 days at 60 °C under vacuum. FTIR (KBr, cm^{-1}): 1712 (C═O); ^{1}H NMR (500 MHz, DMSO–d_6, δ, ppm): 6.40–7.65 (Ar**H**); ^{13}C NMR (125 MHz, DMSO–d_6, δ, ppm): 126.60–140.20 (Ar**C**), 176.35–179.00 (**C**═O); Number–average molecular weight (M_n): ca. 39,000 g mol^{-1} (Fig. S1).

2.4. Polymerization of poly(AS–alt–PMI) and poly(AS–alt–HPMI) copolymers

In a 125 mL two–necked round–bottom flask, either PMI (1.818 g, 10.5 mmol) or HPMI (1.986 g, 10.5 mmol), along with AIBN (5 wt%) were placed. Dry THF (30 mL) and 4–acetoxystyrene (10.5 mmol) were then injected into the flask and the mixture was stirred under N_2 at 70 °C for 1 day. The solution was quenched by exposing to air for half an hour. The solution was added dropwise into cold MeOH and the solid was reprecipitated. The solid was dried for 2 days at 60 °C under vacuum to prevent solvent existing. FTIR (KBr, cm^{-1}): 1711 (C═O); ^{1}H NMR (500 MHz, DMSO–d_6, δ, ppm): 2.20 (C**H**$_3$), 6.25–7.65 (Ar**H**); ^{13}C NMR (125 MHz, DMSO–d_6, δ, ppm): 20.96 (**C**H$_3$), 121.00–138.55 (Ar**C**), 150.53 (**C**OAc), 170.05 (**C**═O, OAc), 175.20–179.45 (**C**═O, maleimide); Number–average molecular weight (M_n): ca. 60,000 g mol^{-1} (Fig. S1) for poly(AS–*alt*–PMI) copolymer. FTIR (KBr, cm^{-1}): 1706 (C═O); ^{1}H NMR (500 MHz, DMSO–d_6, δ, ppm): 2.22 (C**H**$_3$), 6.20–7.50 (Ar**H**), 9.72 (O**H**); ^{13}C NMR (125 MHz, DMSO–d_6, δ, ppm): 20.96 (**C**H$_3$), 114.70–138.30 (Ar**C**), 150.46 (**C**OAc), 158.21 (**C**OH), 170.02 (**C**═O, OAc), 176.20–179.60 (**C**═O, maleimide) for poly(AS–*alt*–HPMI) copolymer. The copolymerization of poly(S–*alt*–HPMI) has been mentioned previously [22].

2.5. Synthesis of poly(VPh–alt–PMI) and poly(VPh–alt–HPMI) copolymers

Poly(AS–*alt*–PMI) copolymer (0.400 g) or poly(AS–*alt*–HPMI) was dissolved by DMF (9 mL) in a 25 mL two necked round–bottom flask under N_2 atmosphere. Deionized water (1 mL) and ammonium ethanoate (0.739 g) were injected into the flask and the solution was stirred at room temperature for 40 h. The solution was added dropwise into cold MeOH and the solid was dried for 3 days at 60 °C under vacuum to remove solvent. FTIR (KBr, cm^{-1}): 1709 (C═O); ^{1}H NMR (500 MHz, DMSO–d_6, δ, ppm): 6.05–7.70 (ArH), 9.42 (OH); ^{13}C NMR (125 MHz, DMSO–d_6, δ, ppm): 114.00–133.80 (Ar**C**), 157.52 (**C**OH),175.80–179.95 (**C**═O) for poly(VPh–*alt*–PMI) copolymer. FTIR (KBr, cm^{-1}): 1706 (C═O); ^{1}H NMR (500 MHz, DMSO–d_6, δ, ppm): 6.10–7.30 (Ar**H**), 9.42 (O**H**, vinyl phenol), 9.75 (O**H**, HPMI); ^{13}C NMR (125 MHz, DMSO–d_6, δ, ppm): 113.80–133.90 (Ar**C**), 157.54 (**C**OH, vinyl phenol), 158.16 (**C**OH, HPMI), 176.00–180.70 (**C**═O) for poly(VPh–*alt*–HPMI) copolymer.

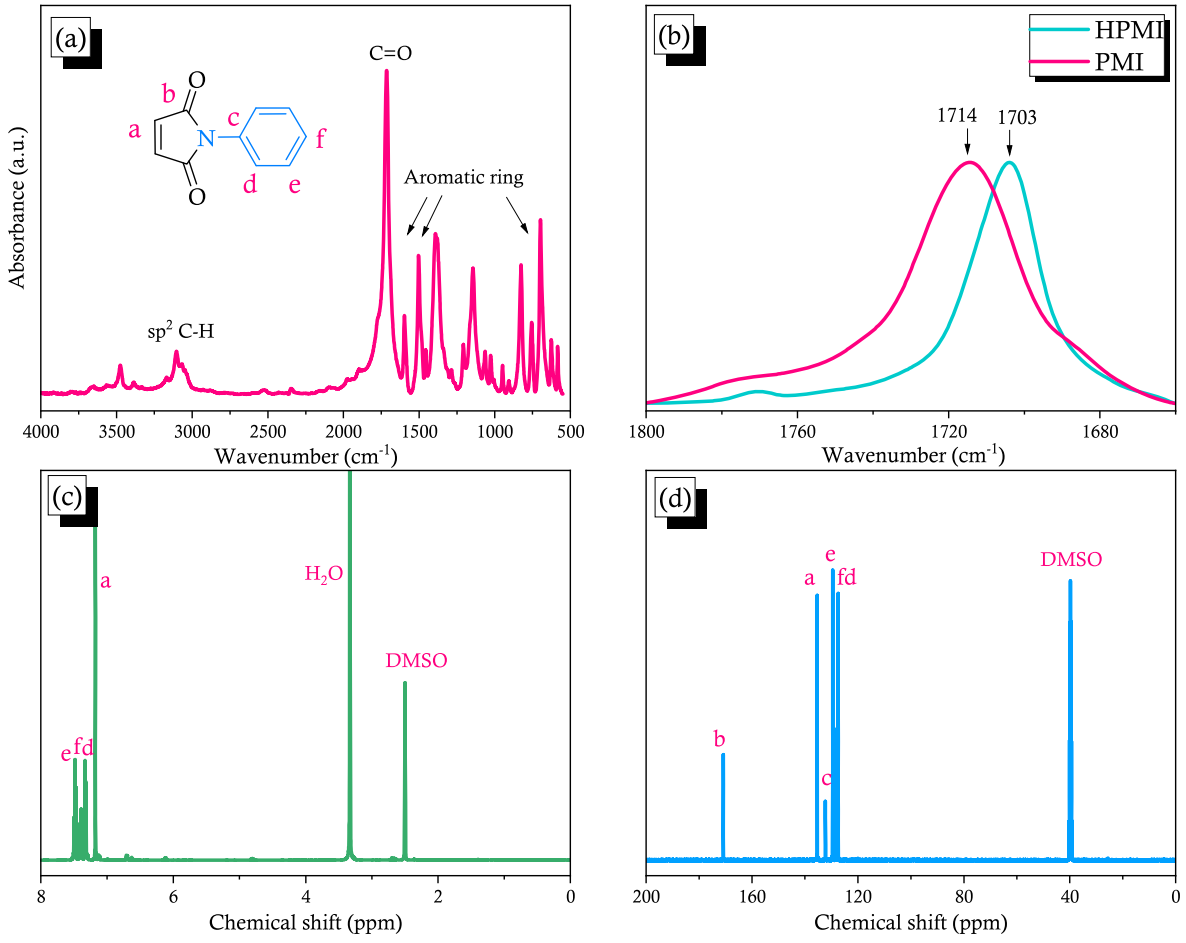

Fig. 1. The synthesis of *N*–phenylmaleimide (PMI): (a) FTIR spectra; (b) Comparison of carbonyl groups between PMI and HPMI; (c) ^{1}H NMR; (d) ^{13}C NMR.

3. Results and discussion

3.1. Synthesis of PMI monomer

We prepared PMI and HPMI monomers to synthesize a series of alternating copolymers based on styrene and phenylmaleimide (PMI) derivative units and those synthetic routes are outlined in Scheme 1. PMI was successfully obtained by reacting from maleic anhydride with aniline where the FTIR spectrum in Fig. 1(a) displays the aromatic ring absorptions at 1503 and 1597 cm^{-1}, the C═O unit at 1714 cm^{-1}, as well as the C–H stretching with sp^2 hybrid at 3000–3200 cm^{-1}, suggesting the successfully synthesis of PMI unit. The FTIR spectrum in Fig. 1(b) shows the C═O absorption of HPMI unit at 1703 cm^{-1} [24], which is much lower wavenumber compared with PMI unit at 1714 cm^{-1}. This reduction in wavenumber can be explained by the occurrence of intermolecular hydrogen bonding between the OH and the C═O group, which could weaken the C═O stretching vibration and the resonance effect also from the phenolic unit would further contribute to the decrease in the wavenumber of the C═O stretching vibration. In addition, the full width at half maximum (FWHM) of PMI is wider, with a value of 32 cm^{-1}, compared to HPMI with a FWHM of 21 cm^{-1} because of most of the HPMI molecule forming the dimers [12], leading to more ordered packing. In contrast, the PMI molecule tends to stack in the disorderly manner because of its nonplanar chemical structure [25] and the weaker intermolecular interaction than that of HPMI unit. Fig. 1(c) displays ^{1}H NMR result where a singlet peak at 7.18 ppm due to the alkene unit, and the peaks at 7.32, 7.39, and 7.48 ppm are corresponding to the aromatic ring signals. ^{13}C NMR spectrum was also used to confirm the aromatic ring, alkene, and C═O units at 127.49–132.26, 135.37, 170.84 ppm as shown in Fig. 1(d), respectively.

3.2. Synthesis of alternating copolymers

We synthesized poly(S–*alt*–PMI), poly(AS–*alt*–PMI), poly(S–*alt*–HPMI), and poly(AS–*alt*–HPMI) copolymers through free radical copolymerization by using styrene and PMI derivatives. The chemical structures of these copolymers were characterized by using FTIR, NMR and MALDI–TOF mass spectra analyses. In FTIR spectra, strong symmetrical C═O vibration of the maleimide units are found at 1712, 1711, and 1706 cm^{-1} for the respective copolymers. Comparing these values to poly(S–*alt*–HPMI) at 1705 cm^{-1}, it is evident that the presence of OH units on the HPMI monomer could influence the C═O vibration, even in the polymerization state. The asymmetrical C═O vibration of these alternating copolymers are found at ca. 1775 cm^{-1} as displayed in Fig. S2. Herein, since the OAc signal at 1763 cm^{-1} [26] was overlapped with asymmetrical C═O stretching of phenylmaleimide units in FTIR spectra of poly(AS–*alt*–PMI) and poly(AS–*alt*–HPMI) copolymers at 1767 cm^{-1}. However, after hydrolysis of poly(AS–*alt*–PMI) and poly(AS–*alt*–HPMI) to form poly(VPh–*alt*–PMI) and poly(VPh–*alt*–HPMI) copolymers, respectively, the asymmetrical C═O vibrations was shift back to ca. 1775 cm^{-1} due to the disappearance of the OAc units. Furthermore, in poly(VPh–*alt*–PMI) copolymer, the appearance of OH signals in the range of 3100–3750 cm^{-1} was observed after hydrolysis from poly(AS–*alt*–PMI) copolymer and becomes broader after hydrolysis

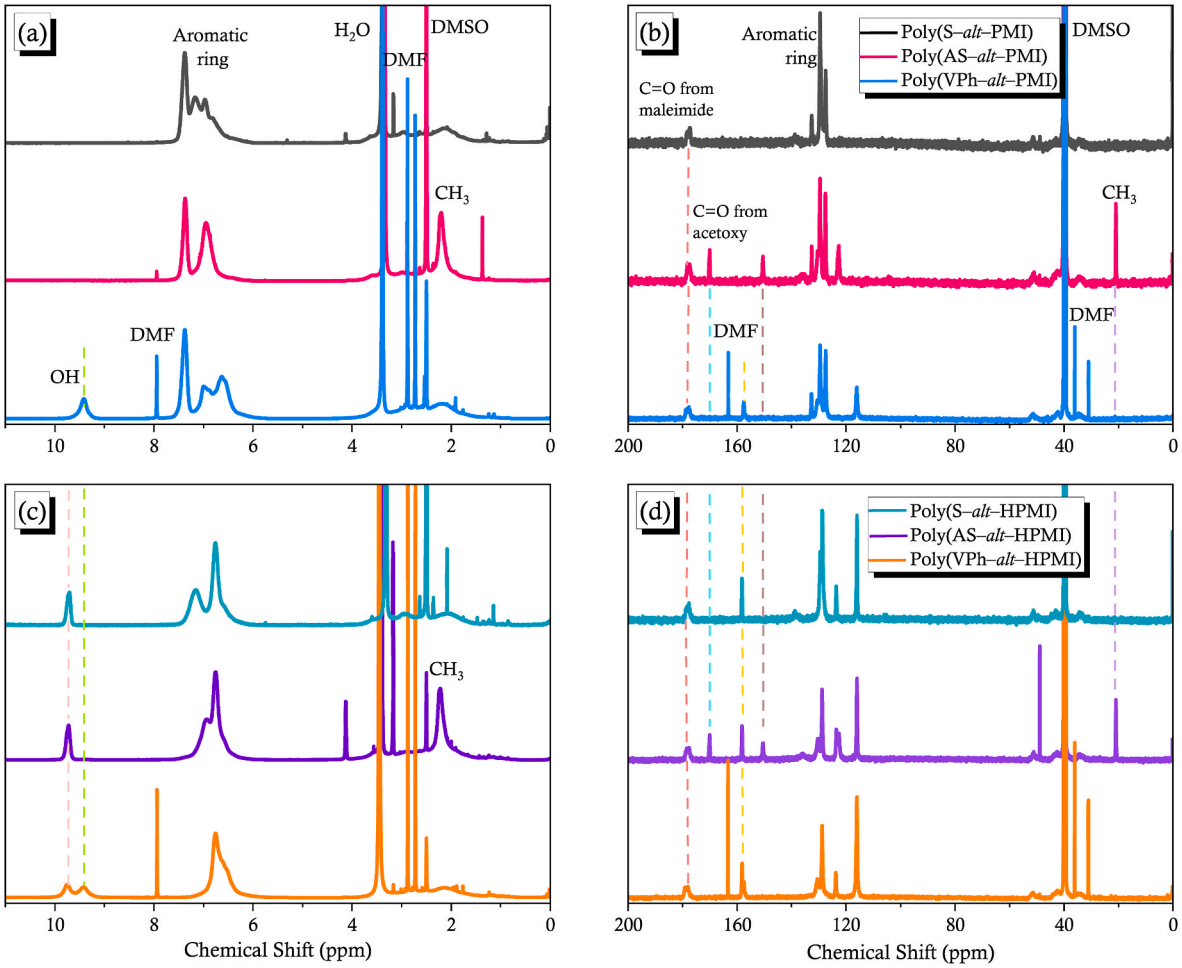

Fig. 2. (a) ^{1}H and (b) ^{13}C NMR of poly(S–*alt*–PMI), poly(AS–*alt*–PMI), and poly(VPh–*alt*–PMI); (c) ^{1}H and (d) ^{13}C NMR of Poly(S–*alt*–HPMI), Poly(AS–*alt*–HPMI), and Poly(VPh–*alt*–HPMI).

of poly(AS–*alt*–HPMI) copolymer to form poly(VPh–*alt*–HPMI) copolymer.

Fig. 2 shows ^{1}H and ^{13}C NMR spectra of these alternating copolymers. The signal of OAc units of poly(AS–*alt*–PMI) at 2.20 ppm was removed and the OH signal was appeared at 9.42 ppm after hydrolysis as shown in Fig. 2(a), confirming the conversion of the OAc to OH units. In Fig. 2(b), the ^{13}C NMR spectra reveals the disappearance of the C═O signal of the OAc unit from poly(AS–*alt*–PMI) copolymer at 170.05 ppm after hydrolysis. In addition, the signal of carbon attached to the acetoxy unit on aromatic ring is shifted from 150.53 to 157.52 ppm upon hydrolysis, also confirming the transformation of the OAc to OH units to form poly(VPh–*alt*–PMI) copolymer. In Fig. 2(c), ^{1}H NMR spectra reveals the distinct signals for the OH unit on the HPMI unit of poly (AS–*alt*–HPMI) at 9.72 ppm, which are located at different positions compared to the signals of the OH unit on the VPh unit. Upon hydrolysis, the signal corresponding to the OAc is replaced with a OH signal at 9.42 ppm, as depicted in Fig. 2(c). Fig. 2(d) illustrates the ^{13}C NMR spectra, displaying that the signal of the OAc unit of poly(AS–*alt*–HPMI) copolymer at 170.02 ppm was disappeared after hydrolysis. Moreover, the signal of the carbon attached to the OAc unit on the aromatic ring shifts from 150.46 to 157.54 ppm, implying the successful hydrolysis of the OAc to the OH group to form poly(VPh–*alt*–HPMI) copolymer.

Characterizing the proton signals on the main chains ranging from 1.45 to 3.85 ppm in the ^{1}H NMR spectra is the challenging because of the overlapping with various solvents. Moreover, the signals of the OAc units at ca. 2.20 ppm are also overlapped and thus to determine the ratio of styrene derivatives to PMI derivatives, the integrals of the aromatic units and OH groups were utilized instead. The repeating unit ratio was calculated from the integration of the ^{1}H NMR spectra, remains the same regardless of whether hydrolysis was performed. For poly(AS–*alt*–PMI) and poly(VPh–*alt*–PMI) copolymers, the styrene derivative (AS and VPh) unit represents for 48.9%, while the PMI unit represents for 51.1%. Similarly, for poly(AS–*alt*–HPMI) and poly(VPh–*alt*–HPMI), the styrene derivative unit accounts 47.1%, while the HPMI unit accounts 52.9%. In addition, as for poly(S–*alt*–HPMI) [22] and poly(S–*alt*–DMHPMI) [27], the styrene unit is 46.5% and 47.9% respectively, whereas the HPMI unit is 53.5% and 52.1%, respectively, were determined in our previous studies, suggesting an alternating tendency in these copolymers, as expected [28]. However, poly(MMA–*co*–HPMI) random copolymers were observed due to a relatively large difference between the reactivity ratios of the two monomers [29]. Notably, there is no specific peak in the ^{1}H NMR analysis of poly(S–*alt*–PMI) copolymer, making it challenging to determine the ratio of repeating units in this specific copolymer.

MALDI–TOF mass spectra could provide additional evidence [30–32] supporting the near–perfectly alternating sequences of these copolymers because of almost equal numbers of styrene derivatives and PMI derivatives in Fig. (3). For example, the signal labeled as "10:10" signifies the presence of 10 units of styrene and 10 units of PMI as shown in Fig. 3(a). The difference between the signals at *m/z* 2871.71 and *m/z* 3149.28 is ca. 277 g mol^{-1}, which is corresponding to the combined mass of one styrene unit (104.15 u) and one PMI unit (173.17 u). The other obvious signals indicate to perfectly alternating sequences with styrene:PMI ratios of *n*–1:*n*, *n*:*n*–1, and *n*:*n* (e.g., 8:9, 9:8, and 9:9, respectively). In addition, a few signals correspond to the ratio of *n*–1:*n*+1, and *n*+1:*n*–1 (e.g., 8:10, and 10:8, respectively), indicating some parts of homo–polymerization were formed. Furthermore, poly

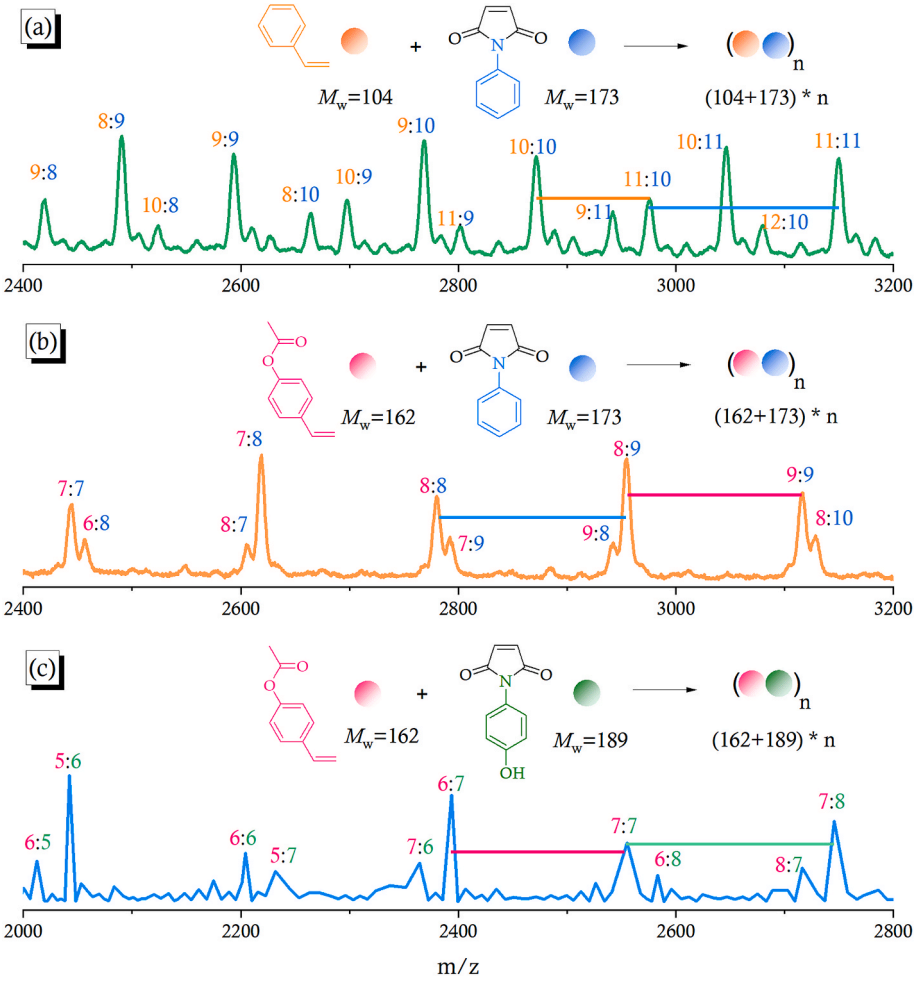

Fig. 3. MALDI TOF Mass spectra of (a) poly(S–*alt*–PMI), (b) poly(AS–*alt*–PMI), (c) poly(AS–*alt*–HPMI).

(AS–*alt*–PMI) was found the difference between the signals at *m/z* 2780.56 and *m/z* 3116.01 is ca. 335 g mol^{-1}, which corresponds to the combined mass of one AS unit (162.19 u) and one PMI unit (173.17 u) as shown in Fig. 3(b). The signal labeled as "8:8″ suggests the presence of 8 units of AS and 8 units of PMI. Similarly, there are other clear signals corresponding to the perfectly alternating sequences with AS:PMI ratios of *n*–1:*n*, *n*:*n*–1, and *n*:*n* such as 7:8, 8:7, and 8:8, respectively and a few signals are due to the ratio of *n*–1:*n*+1 such as 7:9, which arises from homo–copolymerization events once again. Moreover, Fig. 3(c) shows the difference between the signals at *m/z* 2393.90 and *m/z* 2745.38 is ca. 351 g mol^{-1}, which is the sum of one AS unit (162.19 u) and one HPMI unit (189.17 u) in the spectra of poly(AS–*alt*–HPMI) copolymer. The perfectly alternating sequences were observed by the AS:PMI ratios of *n*–1:*n*, *n*:*n*–1, and *n*:*n* such as 5:6, 6:5, and 6:6, respectively. A few signals correspond to the ratio of *n*–1:*n*+1 such as 5:7, showing the present of segments resulting from homo–polymerization. Molecular weight determined from GPC analyses is another important piece of information. Poly(S–*alt*–PMI) and poly(AS–*alt*–PMI) copolymers display single models with number average of molecular weight of ca. 39,000, and 60,000, respectively. However, there are multi–models in copolymers with OH units, because their intramolecular hydrogen bonding interaction can induce chain coil formed as depicted in Fig. S1(b), making inaccurate molecular weight.

3.3. Thermal property of alternating copolymers

To investigate the impact of OH units on the thermal properties of these alternating copolymers, we conducted DSC analyses and determined their intermolecular hydrogen bonding interactions by using FTIR spectra. Fig. 4(a) displays that the T_g value of poly(S–*alt*–PMI) is higher at 217 °C than that of poly(AS–*alt*–PMI) with a T_g value at 200 °C. Since there did not have strong intermolecular interaction in both copolymers, which could attribute to the different of steric hindrance effect. The appearance of acetoxy group in poly(AS–*alt*–PMI) copolymer disrupts the neat stacking of the polymer chain compared with poly (S–*alt*–PMI) copolymer, resulting in an increase of free volume. However, after hydrolysis, intermolecular hydrogen bonding interactions are formed and thus the T_g value of poly(VPh–*alt*–PMI) copolymer dramatically increases by 30 °C compared to poly(AS–*alt*–PMI) copolymer, reaching a value of 230 °C. This significant difference in T_g value is due to the strong hydrogen bonding interactions on the thermal property of alternating copolymers because of the composition heterogeneity effect [18]. In the similar manner, Fig. 4(b) exhibits that the T_g value of poly(AS–*alt*–HPMI) is lower at 244 °C compared to poly (S–*alt*–HPMI) with a T_g value of 259 °C because of the increased free volume of the presence of acetoxy groups; even though the intramolecular hydrogen bonding interaction was occurred between acetoxy and OH group mentioned as summarized in Table 1. Interestingly, the T_g value of poly(VPh–*alt*–HPMI) is lower than poly(AS–*alt*–HPMI) by approximately 30 °C, which is in contrast to the observed trend in poly (VPh–*alt*–PMI) and poly(AS–*alt*–PMI) copolymers. This phenomenon suggests that the occurrence of intramolecular screening effect in poly (VPh–*alt*–HPMI), even the lengths of the repeating units are different. Two hydrogen bonding donor homopolymer blends are usually displayed the negative T_g deviation based on linear rule such as phenolic/phenoxy, PVPh/phenoxy and PVPh/phenolic binary blends because of entropy change increase [33–35]. In addition, the T_g values of these alternating copolymers are over 200 °C, comparing to 168 °C of Poly (4-vinyl phenol) (PVPh) [36] and 122 °C of Poly(4-acetoxystyrene) (PAS) [37] Because maleimide units can restrict the degree of freedom and there is intramolecular screening effect by introducing styrene units alternatingly.

The investigation of these phenomena was conducted by using FTIR spectra as displayed in Fig. 5. The comparison of FWHM between poly (S–*alt*–PMI) and poly(AS–*alt*–PMI) indicates similar values as shown in Table 1, suggesting that the difference in T_g values between these two copolymers is negligibly related to the dipole–dipole moments in poly (AS–*alt*–PMI). In contrast, the FWHM of poly(VPh–*alt*–PMI) is higher of 42.4 cm^{-1} compared to poly(AS–*alt*–PMI) of 23.1 cm^{-1} and the signal shift to 1708 cm^{-1} from 1711 cm^{-1} suggests the presence of strong

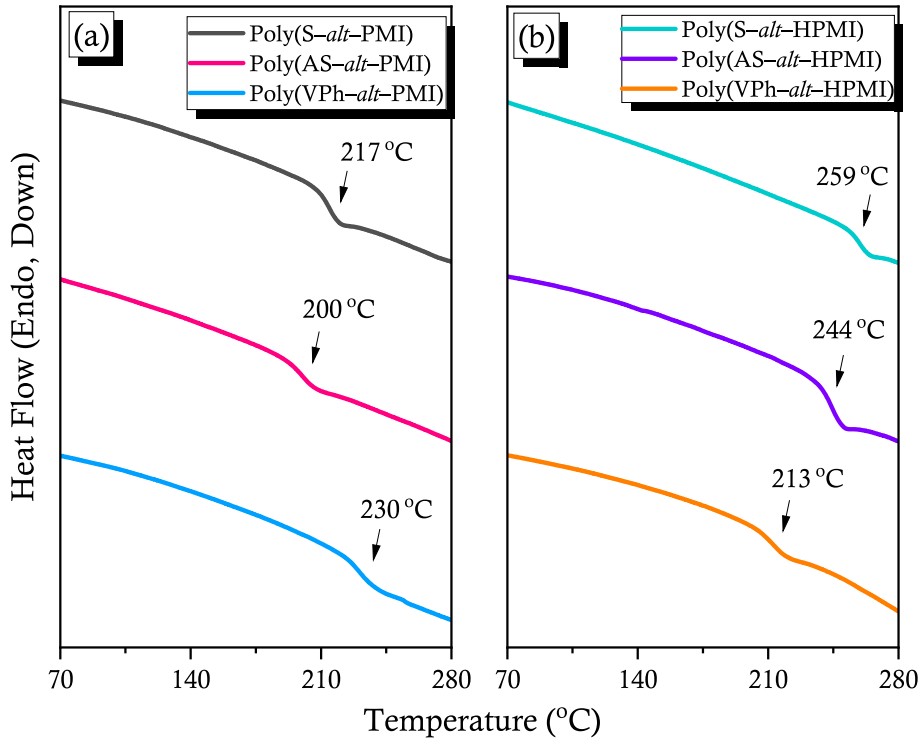

Fig. 4. DSC results for (a) PMI derivative alternating copolymers and (b) HPMI derivative alternating copolymers, were recorded at 2nd heating cycle to remove residue.

Table 1
The ratio of H–bonded C═O and their thermal property of these alternating copolymers synthesized in this study.

	FWHM of C═O on maleimide (cm^{-1})	H–bonded C═O on OAc (%)[a]	H–bonded C═O on maleimide (%)[a]	Peak of H-bonded multimer (cm^{-1})[b]	T_g (°C)
Poly(S–*alt*–PMI)	23.6	–	–	–	217
Poly(AS–*alt*–PMI)	23.1	–	–	–	200
Poly(VPh–*alt*–PMI)	42.4	–	38.6	3223	230
Poly(S–*alt*–HPMI)	40.5	–	40.4	3302	259
Poly(AS–*alt*–HPMI)	46.3	48.4	45.6	3283	244
Poly (VPh–*alt*–HPMI)	43.4	–	47.0	3150	213

[a] Peak fitting are shown on Fig. S3.
[b] The peaks are from Fig. 6.

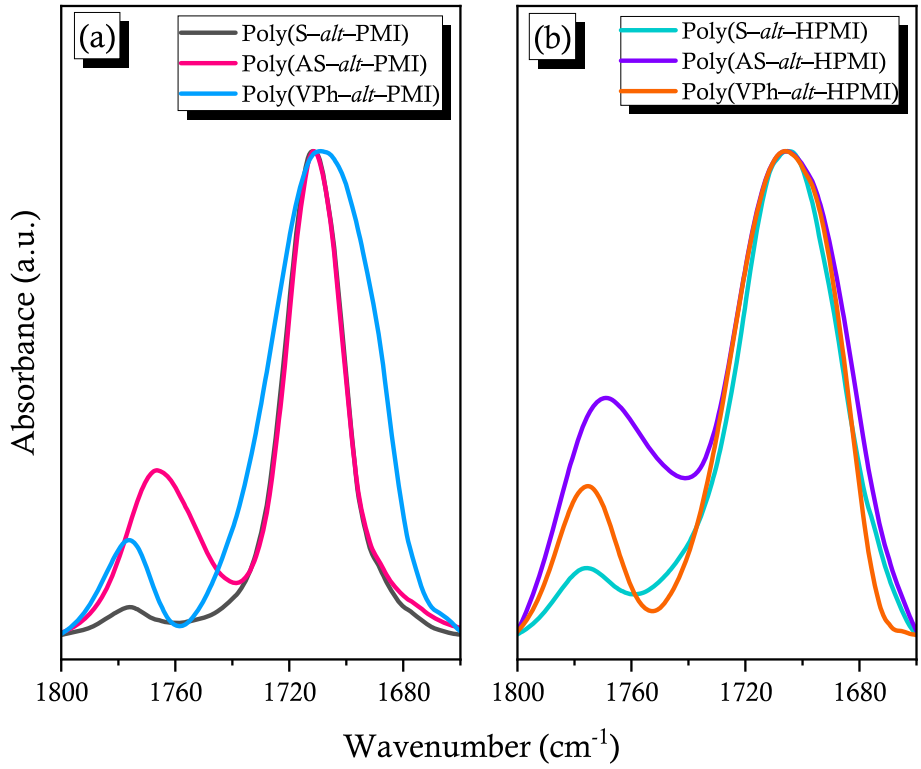

Fig. 5. FTIR spectra of carbonyl stretching of (a) PMI derivative alternating copolymers and (b) HPMI derivative alternating copolymers.

intermolecular hydrogen bonding interaction in poly(VPh–*alt*–PMI), contributing significantly to the remarkable increase in value of T_g. Interestingly, despite both poly(VPh–*alt*–PMI) and poly(S–*alt*–HPMI) containing only one OH units, there is a difference in T_g values of ca. 20 °C.

Upon simulation, it was found that the stacking of alternating copolymer chains allows for ready interaction between HPMI units, which could account for this difference [22]. On the other hand, the presence of acetoxy group in poly(AS–*alt*–HPMI) increase the mobility of copolymer chain even though the potential for interaction between two types of C═O could interact with OH group. It is quite surprising that poly(VPh–*alt*–HPMI), which has two OH groups on both styrene and PMI units, but exhibits the lowest T_g value. We found the overall intermolecular hydrogen bonding interaction decreasing in Table 1, could be attributed to a slight increase in the ratio of hydrogen bonded C═O on the maleimide unit, while the acetoxy unit has been hydrolyzed. Moreover, to confirm the presence of intramolecular hydrogen bonding interaction between OH and OH groups, it is important to understand the correlation between them. The 2D–FTIR spectral analysis method, established by Noda et al. [38], has been widely applied [36,39–41]. This characterization could be allowed for the understanding of 2D synchronous FTIR spectra, which display symmetry along the diagonal line the correlation map. By inducing environmental perturbation, auto peaks are generated, and the positive signal by red color can be obtained. Cross–peaks could be observed at the off–diagonal position, and the negative signal (blue color) imply the intensity fluctuations of the two peaks at ν_1 and ν_2 under environmental perturbation would vary in opposite directions. Fig. 6 displays 2D synchronous FTIR spectral map of alternating copolymers with OH groups. Free OH stretching signals are at ca. 3650 cm^{-1}, hydrogen bonded dimer, trimer, and others are located at ca. 3550 cm^{-1} [10]. The signals of hydrogen bonded multimer below 3430 cm^{-1}, and thus the cross–peaks were negative correlation displayed in Fig. 6. Using subjecting the hydrogen bonded multimers to high temperatures, they undergo dissociation of hydrogen bonding interaction as shown in Fig. S4. Furthermore, the lower wavenumber presents a high presence of hydrogen bonded multimers, as the strength of the OH vibration is diminished by other OH groups. The specific wavenumbers associated with hydrogen bonded multimers are as follows: 3223 cm^{-1} for poly(VPh–*alt*–PMI), 3302 cm^{-1} for poly (S–*alt*–HPMI), 3283 cm^{-1} for poly(AS–*alt*–HPMI), and 3150 cm^{-1} for poly(VPh–*alt*–HPMI) copolymer. Interestingly, this trend aligns perfectly with the T_g values displayed in Table 1, suggesting that a

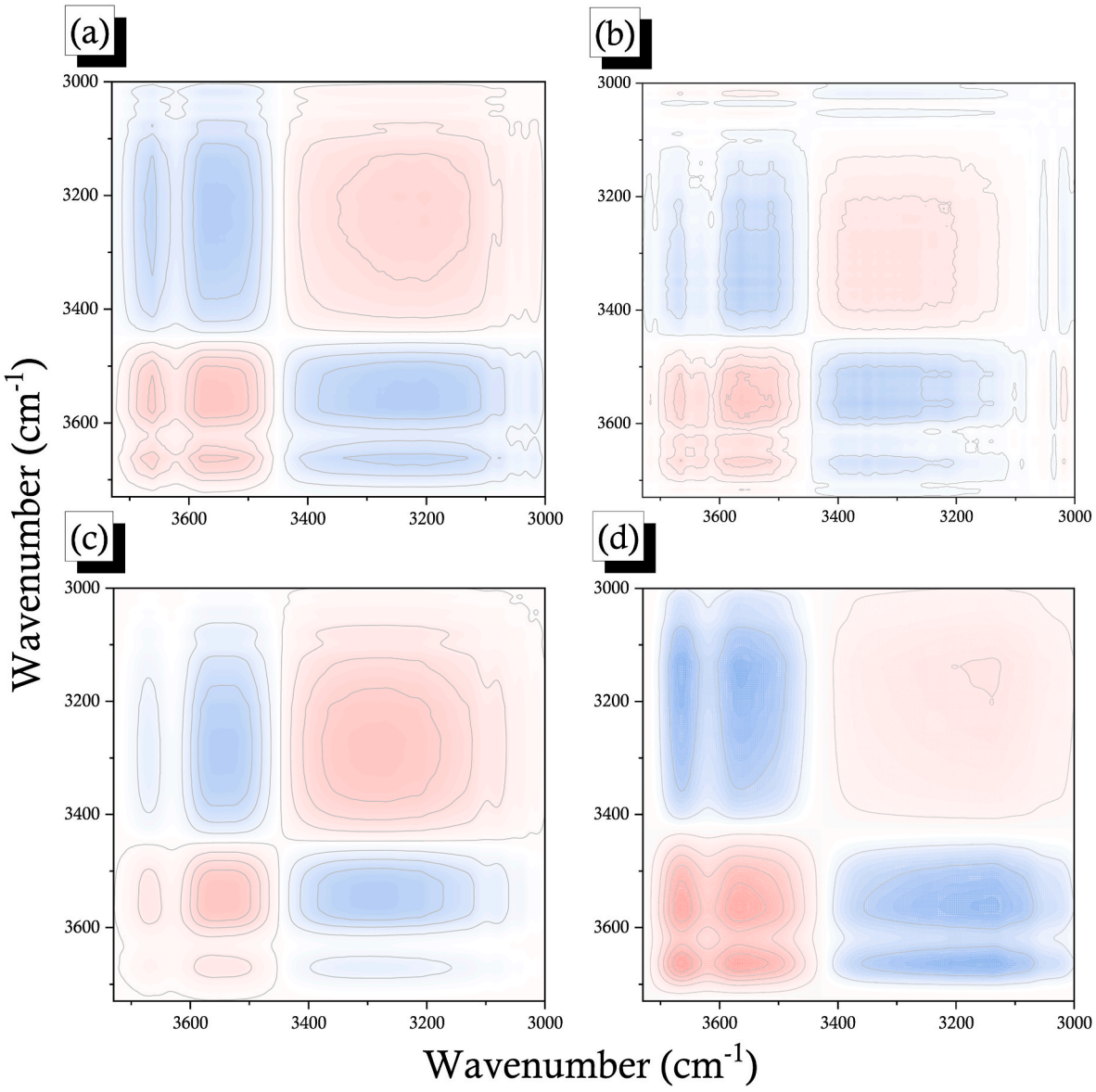

Fig. 6. 2D synchronous FTIR of hydroxyl stretching of (a) Poly(VPh–*alt*–PMI); (b) Poly(S–*alt*–HPMI); (c) Poly(AS–*alt*–HPMI); (d) Poly(VPh–*alt*–HPMI).

greater presence of hydrogen bonded multimers leads to strong intramolecular hydrogen bonding interactions within these copolymers. Notably, the lowest wavenumber of poly(VPh–*alt*–HPMI) was observed, indicating the intramolecular screening effect made a pronounced influence on T_g behavior.

4. Conclusions

Strong hydrogen bonding interactions and higher T_g values were discovered in the single OH group on each repeating unit of alternating copolymers through the characterization by MALDI–TOF mass and ^{1}H NMR spectra, suggesting that the introduction of each inert diluent segment between hydrogen bonding donors segment could enhance intermolecular hydrogen bonding interactions of poly(VPh–*alt*–PMI) or poly(S–*alt*–HPMI). In contrast, poly(VPh–*alt*–HPMI), with two hydrogen bonding donors without inert diluent segment introducing, would cause serious intramolecular screening effect, as confirmed by 2D–FTIR spectral analyses. This effect leads to the decrease in the T_g value. It provides that only the presence of hydrogen bonding but also the free volume plays an important role in the effect of the T_g behavior of poly (S–*alt*–HPMI) copolymer. As a result, the significance of hydrogen bonding interaction, the presence of inert diluent PS or PMI segment, and free volume from acetoxy group are in determining the T_g values of these alternating copolymers.

CRediT authorship contribution statement

Wei-Ting Du: Methodology, Synthesis, Investigation, Formal analysis, Writing – original draft. **Shiao-Wei Kuo:** Supervision, Writing – original draft, Writing – review & editing.

Declaration of competing interest

The authors declare that they have no known competing financial interests or personal relationships that could have appeared to influence the work reported in this paper.

Data availability

The data that has been used is confidential.

Acknowledgments

This study was supported financially by the National Science and Technology Council, Taiwan, under contracts NSTC 110-2124-M-002-013 and 111-2223-E-110-004.

Appendix A. Supplementary data

Supplementary data to this article can be found online at https://doi.org/10.1016/j.polymer.2023.126382.

References

[1] Y. Ye, S. Xian, H. Cui, K. Tan, L. Gong, B. Liang, T. Pham, H. Pandey, R. Krishna, P.-C. Lan, K.A. Forrest, B. Space, T. Thonhauser, J. Li, S. Ma, Metal−Organic framework based hydrogen-bonding nanotrap for efficient acetylene storage and separation, J. Am. Chem. Soc. 144 (2022) 1681–1689, https://doi.org/10.1021/jacs.1c10620.

[2] X. Song, Y. Wang, C. Wang, D. Wang, G. Zhuang, K.O. Kirlikovali, P. Li, O.K. Farha, Design rules of hydrogen-bonded organic frameworks with high chemical and thermal stabilities, J. Am. Chem. Soc. 144 (2022) 10663–10687, https://doi.org/10.1021/jacs.2c02598.

[3] L.A. Galuska, M.U. Ocheje, Z.C. Ahmad, S. Rondeau-Gagné, X. Gu, Elucidating the role of hydrogen bonds for improved mechanical properties in a high-performance semiconducting polymer, Chem. Mater. 34 (2022) 2259–2267, https://doi.org/10.1021/acs.chemmater.1c04055.

[4] A.S. Mora, R. Tayouo, B. Boutevin, G. David, S. Caillol, A perspective approach on the amine reactivity and the hydrogen bonds effect on epoxy-amine systems, Eur. Polym. J. 123 (2020), 109460, https://doi.org/10.1016/j.eurpolymj.2019.109460.

[5] M.G. Mohamed, W.C. Chang, S.W. Kuo, Crown ether- and benzoxazine-linked porous organic polymers displaying enhanced metal ion and CO2 capture through solid-state chemical transformation, Macromolecules 55 (2022) 7879–7892, https://doi.org/10.1021/acs.macromol.1c00736.

[6] X. Li, Y. He, X. Dong, X. Ren, H. Gao, W. Hu, Effects of hydrogen-bonding density on polyamide crystallization kinetics, Polymer 189 (2020), 122165, https://doi.org/10.1016/j.polymer.2020.122165.

[7] Y. Eom, S.M. Kim, M. Lee, H. Jeon, J. Park, E.S. Lee, S.Y. Hwang, J. Park, D.X. Oh, Mechano-responsive hydrogen-bonding array of thermoplastic polyurethane elastomer captures both strength and self-healing, Nat. Commun. 12 (2021) 621, https://doi.org/10.1038/s41467-021-20931-z.

[8] S.W. Kuo, Hydrogen Bonding in Polymeric Materials, John Wiley & Sons, 2018.

[9] S.W. Kuo, Hydrogen bonding interactions in polymer/polyhedral oligomeric silsesquioxane nanomaterials, J. Polym. Res. 29 (2022) 69, https://doi.org/10.1007/s10965-021-02885-4.

[10] Y. Deng, Q. Zhang, C. Shi, R. Toyoda, D. Qu, H. Tian, B.L. Feringa, Acylhydrazine-based reticular hydrogen bonds enable robust, tough, and dynamic supramolecular materials, Sci. Adv. 8 (2022), https://doi.org/10.1126/sciadv.abk3286 eabk3286.

[11] M.M. Coleman, P.C. Painter, Hydrogen bonded polymer blends, Prog. Polym. Sci. 20 (1995) 1–59, https://doi.org/10.1016/0079-6700(94)00038-4.

[12] S.W. Kuo, S.C. Chan, F.C. Chang, Effect of hydrogen bonding strength on the microstructure and crystallization behavior of crystalline polymer blends, Macromolecules 36 (2003) 6653–6661, https://doi.org/10.1021/ma034695a.

[13] S.W. Kuo, Construction Archimedean tiling patterns based on soft materials from block copolymers and covalent organic frameworks, Giant 15 (2023), 100170, https://doi.org/10.1016/j.giant.2023.100170.

[14] Y.C. Huang, W.C. Chen, S.W. Kuo, Mesoporous phenolic/POSS hybrids induced by microphase separation arising from competitive hydrogen bonding interactions, Macromolecules 55 (2022) 8918–8930, https://doi.org/10.1021/acs.macromol.2c01585.

[15] T.C. Chou, W.C. Chen, M.G. Mohamed, Y.C. Huang, S.W. Kuo, Organic-inorganic phenolic/POSS hybrids provide highly ordered mesoporous structures templated by high thermal stability of PS-b-P4VP diblock copolymer, Chem. Eur J. 29 (2023), e202300538, https://doi.org/10.1002/chem.202300538.

[16] T.C. Tseng, S.W. Kuo, Hydrogen-bonding strength influences hierarchical self-assembled structures in unusual miscible/immiscible diblock copolymer blends, Macromolecules 51 (2018) 6451–6459, https://doi.org/10.1021/acs.macromol.8b00751.

[17] C.L. Lin, W.C. Chen, C.S. Liao, Y.C. Su, C.F. Huang, S.W. Kuo, F.C. Chang, Sequence distribution and polydispersity index affect the hydrogen-bonding strength of poly (vinylphenol-co-methyl methacrylate) copolymers, Macromolecules 38 (2005) 6435–6444, https://doi.org/10.1021/ma050639t.

[18] M.M. Coleman, Y. Xu, P.C. Painter, Compositional heterogeneities in hydrogen-bonded polymer blends: infrared spectroscopic results, Macromolecules 27 (1994) 127–134, https://doi.org/10.1021/ma00079a019.

[19] P.C. Painter, B. Veytsman, S. Kumar, S. Shenoy, J.F. Graf, Y. Xu, M.M. Coleman, Intramolecular screening effects in polymer mixtures. 1. Hydrogen-bonded polymer blends, Macromolecules 30 (1997) 932–942, https://doi.org/10.1021/ma960815l.

[20] M.M. Coleman, P.C. Painter, Intramolecular screening and functional group accessibility effects in polymer blends: the prediction of phase behavior, Macromol. Chem. Phys. 199 (1998) 1307–1314, https://doi.org/10.1002/(SICI)1521-3935(19980701)199:7<1307::AID-MACP1307>3.0.CO;2-%23.

[21] W.C. Chen, R.C. Lin, S.M. Tseng, S.W. Kuo, Minimizing the strong screening effect of polyhedral oligomeric silsesquioxane nanoparticles in hydrogen-bonded random copolymers, Polymers 10 (2018) 303, https://doi.org/10.3390/polym10030303.

[22] W.T. Du, E.A. Orabi, M.G. Mohamed, S.W. Kuo, Inter/intramolecular hydrogen bonding mediate miscible blend formation between near-perfect alternating Poly (styrene-alt- hydroxyphenylmaleimide) copolymers and Poly(vinyl pyrrolidone), Polymer 219 (2021), 123542, https://doi.org/10.1016/j.polymer.2021.123542.

[23] A. Prinos, A. Dompros, C. Panayiotou, Thermoanalytical and spectroscopic study of poly(vinyl pyrrolidone)/poly(styrene-co-vinyl phenol) blends, Polymer 39 (1998) 3011–3016, https://doi.org/10.1016/S0032-3861(97)10085-4.

[24] S.W. Kuo, F.C. Chang, Studies of miscibility behavior and hydrogen bonding in blends of poly(vinylphenol) and poly(vinylpyrrolidone), Macromolecules 34 (2001) 5224–5228, https://doi.org/10.1021/ma010517a.

[25] S. Terada, A. Matsumoto, Role of N-substituents of maleimides on penultimate unit effect for sequence control during radical copolymerization, Polym. J. 51 (2019) 1137–1146, https://doi.org/10.1038/s41428-019-0227-y.

[26] S.W. Kuo, F.C. Chang, Effect of copolymer composition on the miscibility of poly (styrene-co-acetoxystyrene) with phenolic resin, Polymer 42 (2001) 9843–9848, https://doi.org/10.1016/S0032-3861(01)00526-2.

[27] W.-T. Du, T.-L. Ma, S.-W. Kuo, Steric hindrance affects interactions of poly (styrene–alt–DMHPMI) copolymer with strongly hydrogen-bond-accepting homopolymers, Polymer 268 (2023), 125694, https://doi.org/10.1016/j.polymer.2023.125694.

[28] G. Odian, Principles of Polymerization, Wiley, New York, 2004, https://doi.org/10.1002/047147875X.

[29] W.T. Du, S.W. Kuo, Varying the sequence distribution and hydrogen bonding strength provides highly Heat-Resistant PMMA copolymers, Eur. Polym. J. 170 (2022), 111165, https://doi.org/10.1016/j.eurpolymj.2022.111165.

[30] K. Nishimori, M. Ouchi, M. Sawamoto, Sequence analysis for alternating copolymers by MALDI-TOF-MS: importance of initiator selectivity for comonomer pair, Macromol. Rapid Commun. 37 (2016) 1414–1420, https://doi.org/10.1002/marc.201600251.

[31] M.G. Mohamed, K.-C. Hsu, J.-L. Hong, S.-W. Kuo, Unexpected fluorescence from maleimide-containing polyhedral oligomeric silsesquioxanes: nanoparticle and sequence distribution analyses of polystyrene-based alternating copolymers, Polym. Chem. 7 (2016) 135, https://doi.org/10.1039/c5py01537e.

[32] J.S. Town, G.R. Jones, D.M. Haddleton, MALDI-LID-ToF/ToF analysis of statistical and diblock polyacrylate copolymers, Polym. Chem. 9 (2018) 4631–4641, https://doi.org/10.1039/c8py00928g.

[33] S.W. Kuo, C.L. Lin, H.D. Wu, F.C. Chang, Thermal property and hydrogen bonding in blends of poly (vinylphenol) and poly (hydroxylether of bisphenol A), J. Polym. Res. 10 (2003) 87–93, https://doi.org/10.1023/A:1024997309640.

[34] S.W. Kuo, S.C. Chan, H.D. Wu, F.C. Chang, An unusual, completely miscible, ternary hydrogen-bonded polymer blend of phenoxy, phenolic, and PCL, Macromolecules 38 (2005) 4729–4736, https://doi.org/10.1021/ma047371a.

[35] S.W. Kuo, The totally miscible in ternary hydrogen-bonded polymer blend of poly (vinyl phenol)/phenoxy/phenolic, J. Appl. Polym. Sci. 114 (2009) 116–124, https://doi.org/10.1002/app.30490.

[36] W.T. Du, Y.L. Kuan, S.W. Kuo, Intra- and intermolecular hydrogen bonding in miscible blends of CO2/epoxy cyclohexene copolymer with poly(vinyl phenol), Int. J. Mol. Sci. 23 (2022) 7018, https://doi.org/10.3390/ijms23137018.

[37] S.W. Kuo, W.P. Liu, F.C. Chang, Miscibility enhancement on the immiscible binary blend of poly(vinyl phenol) and poly(acetoxystyrene) with poly(ethylene oxide), Macromol. Chem. Phys. 206 (2005) 2307–2315, https://doi.org/10.1002/macp.200500334.

[38] I. Noda, Y. Ozaki, Two-Dimensional Correlation Spectroscopy, John Wiley & Sons, Hoboken, NJ, USA, 2004, https://doi.org/10.1002/0470012404.

[39] R. Hu, X. Ding, P. Yu, X. He, A. Watts, X. Zhao, J. Wang, Ultrafast two-dimensional infrared spectroscopy resolved a structured lysine 159 on the cytoplasmic surface of the microbial photoreceptor bacteriorhodopsin, J. Am. Chem. Soc. 144 (2022) 22083–22092, https://doi.org/10.1021/jacs.2c09435.

[40] H.T. Kratochvil, J.K. Carr, K. Matulef, A.W. Annen, H. Li, M. Maj, J. Ostmeyer, A. L. Serrano, H. Raghuraman, S.D. Moran, J.L. Skinner, E. Perozo, B. Roux, F. I. Valiyaveetil, M.T. Zanni, Instantaneous ion configurations in the K+ ion channel selectivity filter revealed by 2D IR spectroscopy, Science 353 (2016) 1040–1044, https://doi.org/10.1126/science.aag1447.

[41] S.W. Kuo, H.C. Lin, W.J. Huang, C.F. Huang, F.C. Chang, Hydrogen bonding interactions and miscibility between phenolic resin and octa (acetoxystyryl) polyhedral oligomeric silsesquioxane (AS-POSS) nanocomposites, J. Polym. Sci., Part B: Polym. Phys. 44 (2006) 673–686, https://doi.org/10.1002/polb.20731.